QIRT'2022
10.21611/qirt.2022.2006
16th Quantitative InfraRed Thermography Conference

Parametric study of excitation and processing parameters applied to composites parts using analytic calculation

by S. Maillard*, V. Blouin*, A. Baillard**

* Safran Composites, 33 avenue de la gare, 91760 Itteville, France, samuel.maillard@safrangroup.com
** Safran Nacelles, 4039 Port du Havre, 76700 Gonfreville l'OrcherFrance, andre.baillard@safrangroup.com

Abstract

In order to develop infrared inspection for aerospace sandwich components, a better knowledge of the key parameters of the process was required. Thus, analytic calculations were used to have a better understanding of acquisition and processing parameters.

The results are analysed and compared with elements given in the bibliography in the terms of amplitude, CNR and characteristics times on the curves.

They allowed Safran to select the more suitable configuration to inspect composites panel and define acquisition parameters (energy deposited, acquisition duration,…) to be used regarding the material diffusivity and thickness.

1. Introduction

Aerospace sandwich components are commonly inspected using waterjet through transmission ultrasonic testing. In the frame of R&D activities about composites inspection, Safran investigated alternative methods such as infrared thermography for an industrial application on nacelles components.

To be applied for aerospace applications, the influence of key parameters of the process has to be demonstrated experimentally and, if possible, using simulations. Thus, analytic calculations were used to increase our knowledge about this new method and have a better understanding of acquisition and processing parameters.

2. Model used

In the early 2000, Jean-Yves Marin (Dassault Aviation - IRT Level 3 according to EN4179) created a software called ITsimul2 [1] based on thermal calculation of heat diffusion through a material (sound or with a defect) using a one dimension model, i.e. radial thermal properties are not taken into account. The other assumptions are:

- Thermal excitation uniform on the surface of the material,
- Thermal exchanges with environment uniform on the surface of the material (with ambient air),
- Initial temperature homogeneous through the material and equals to ambient temperature,
- Thermal properties homogeneous on the thickness of each material.

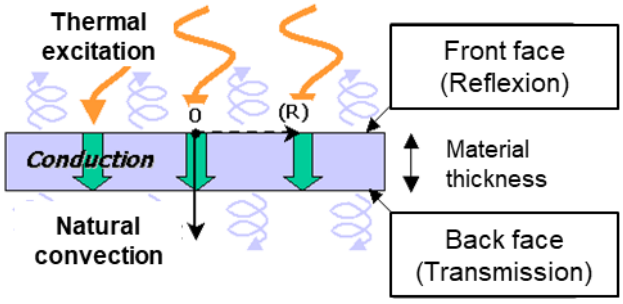

Fig. 1. *Principle of the calculation in ITsimul2 [1]*

This software allows evaluating the influence of many parameters of the process:
- Material (thickness, thermal diffusivity and conductivity),
- Defect characteristics (delamination opening and depth),
- Excitation source (lock-in, step heating and pulse - static or dynamic) and energy deposited,
- Natural convection.

The model allows to calculate instantaneous temperature on both surfaces of the material with a user defined step of time. As this study was focused to understand behaviour in reflexion, only result on front face were analysed.

As shown in Table 1, many parameters were tested. This paper is focused on the influence of material thickness, defect thickness and energy deposited.

	Parameter		Default value	Variation range
Material (CFRP)	Thermal diffusivity	α	$5.3 \times 10^{-7}\ \mathrm{m^2/s}$	$[2,8] \times 10^{-7}\ \mathrm{m^2/s}$
	Thermal conductivity	λ	$0.558\ \mathrm{W.m^{-1}.K^{-1}}$	$[0.05,2]\ \mathrm{W.m^{-1}.K^{-1}}$
	Thickness	**L**	**3 mm**	$\mathbf{[0.9,15]}$ **mm**
Defect (delamination)	Thickness	**Ep**	**25 µm**	$\mathbf{[6.25,100]}$ **µm**
	Thermal conductivity	$\lambda_{def} =$	$0.024 W.m^{-1}.K^{-1}$	-
Heating device	Flash	$\mathbf{Q_c}$	$\mathbf{4\ kJ/m^2}$	$\mathbf{[1,20]\ kJ/m^2}$
		t_c	10 ms	-
	Lock-In	$\mathbf{Q_c}$	$\mathbf{4\ kW/m^2}$	$\mathbf{[1,20]\ kW/m^2}$
		$[f_{min}, f_{max}]$	[0.0125,25]Hz	-
Ambient environment	Ambient temperature	$T(t_0)$	20 °C	-
	Convection	h	$10\mathrm{W.m^{-2}K^{-1}}$	$[5,50]\ \mathrm{W.m^{-2}K^{-1}}$

Table 1. *Default and range of values used for the parametric study*

3. Metric

The results from these calculations were analysed using different metrics described below.

3.1. Absolute contrast

A very common method to compare signals between a sound and a defective area is to estimate the contrast [2]. In this study, the absolute contrast is calculated according to Eq. (1) and used for flash or step heating excitation. An example is given in figure 2.

$$C^a(t) = \Delta T(t) = T_{def}(t) - T_s(t) \quad (1)$$

With:
- T_s : Temperature on a sound area (*K* or °*C*)
- T_{def} : Temperature on a defective zone (*K* or °*C*)
- t_0 : Initial time, just before the flash (*s*)
- t : Elapsed time after flash (s)

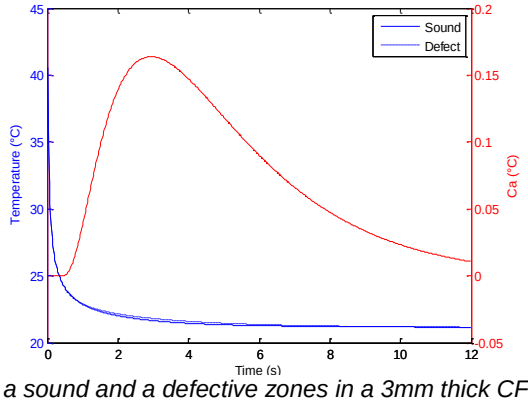

Fig. 2. *Typical thermal behaviour for a sound and a defective zones in a 3mm thick CFRP plate after flash excitation and associated instantaneous absolute contrast*

3.2. Relationship between depth of the defect and maximum of contrast

Many studies have been performed to find the relationship between this contrast evolution (especially the time of *maximum contrast* t_{cmax} and the depth of the defect z). 2 different formulas are used in this study. Eq. (2) is referenced as $t_{cmax\,(theo)}(Cielo\ et\ al.,1987a)$ [3] and Eq. (3) is referenced as $t_{cmax\,(theo)}(Maldague,1993)$ [2];

$$Z \approx \sqrt{t_{cmax} \times \alpha} \quad (2)$$

$$t_{cmax} = 1.705 + 1.881 \times Z + 0.921 \times Z^2 + 0.000799 \times Z \times R_{def} + 0.00138 \times R_{def} - 8.164 \times 10^{-9} R_{def}^2 \quad (3)$$

With : - z: Depth of the defect *(m)*
- α: Material thermal diffusivity (m^2/s)
- $\mathrm{R_{def}} = \frac{\mathrm{Ep}}{\lambda_{\mathrm{def}}}$: Thermal resistance of the defect.

3.3. Lock-in [4]

Lock-in is a well-known excitation technique [4] based on a periodical energy deposit on the surface of the material to analyse. For composites applications, heat source is usually sine modulated halogen lamps.

For a material with a thermal diffusivity $\alpha\ (m^2/s)$ heated at a frequency $f_{LI}\ (Hz)$, inspected thickness L *(m)* is equivalent to the thermal diffusion length and is given by equation (4).

$$\mathrm{L} = \sqrt{\frac{\alpha}{\pi \times \mathrm{f_{LI}}}} \qquad (4)$$

In this technique, the amplitude and phase values between excitation source and thermal behaviour are computed. Figure 3 presents a typical phase contrast signal obtained between a sound 3mm thick CFRP zone and a zone with a defect located at the middle of the thickness excited with frequencies between 0.01 and 2*Hz*.

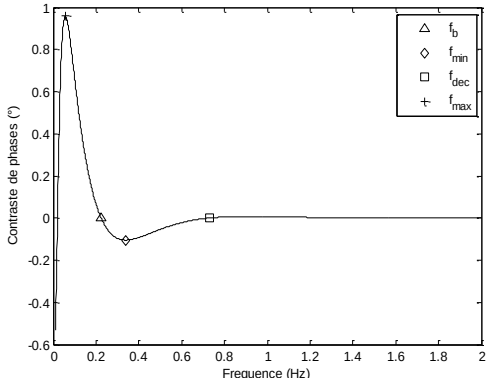

Fig. 3. *Phase contrast evolution according to lock-in frequency*

Between sound areas, phase contrast would remain equal to 0 whatever the excitation frequency. On a zone with a defect, contrast changes with frequencies.

According to [5], frequency $\mathrm{f_b}\ (Hz)$, where contrast goes from a negative to a positive value, is called blind frequency and is linked to the depth of the defect z by the relationship given in Eq. (5).

$$\mathrm{Z} = \mathrm{C_1} \times \sqrt{\frac{\alpha}{\pi.\mathrm{f_b}}} \approx \sqrt{\frac{\alpha}{\mathrm{f_b}}} \qquad (5)$$

With: - $C_1 \approx 1.8 \approx \sqrt{\pi}$

Another interesting point can be noted: f_{dec} corresponding to the frequency when phase contrast starts be different than 0 for decreasing lock-in frequencies.

3.4. PPT

By extension to lock-in, since a flash excitation can be assumed as Dirac pulse, Fast Fourier Transform can be applied on thermal data obtained after flash. Amplitude and phase can be estimated for a range of frequencies depending on acquisition duration and acquisition frequencies. The use of phase images allows canceling inhomogeneities due to flash excitation and makes the analysis easier. This technique is known as PPT, for Pulse Phase Thermography [5]. Like in lock-in (cf. figure 3), phase contrast can be calculated and the same characteristics points can be observed.

3.5. TSR

In the earlies 2000, a new signal processing called ThermoSignal Reconstruction (TSR) has been proposed [6]. Based on a fitting of the logarithmic temporal behavior of the material in the logarithmic domain, it allows to calculate the first and the second derivative (respectively noted *1D* and *2D*) of the heat propagation within the material (cf. figure 4). Such a processing is interesting since it allows an early detection of the defect within the material.

When using TSR, the time of the maximum of the second derivative signal is a characteristic time called $t^* = \frac{L^2}{\pi.\alpha}$,linked to the thickness of the material L and its thermal diffusivity α.

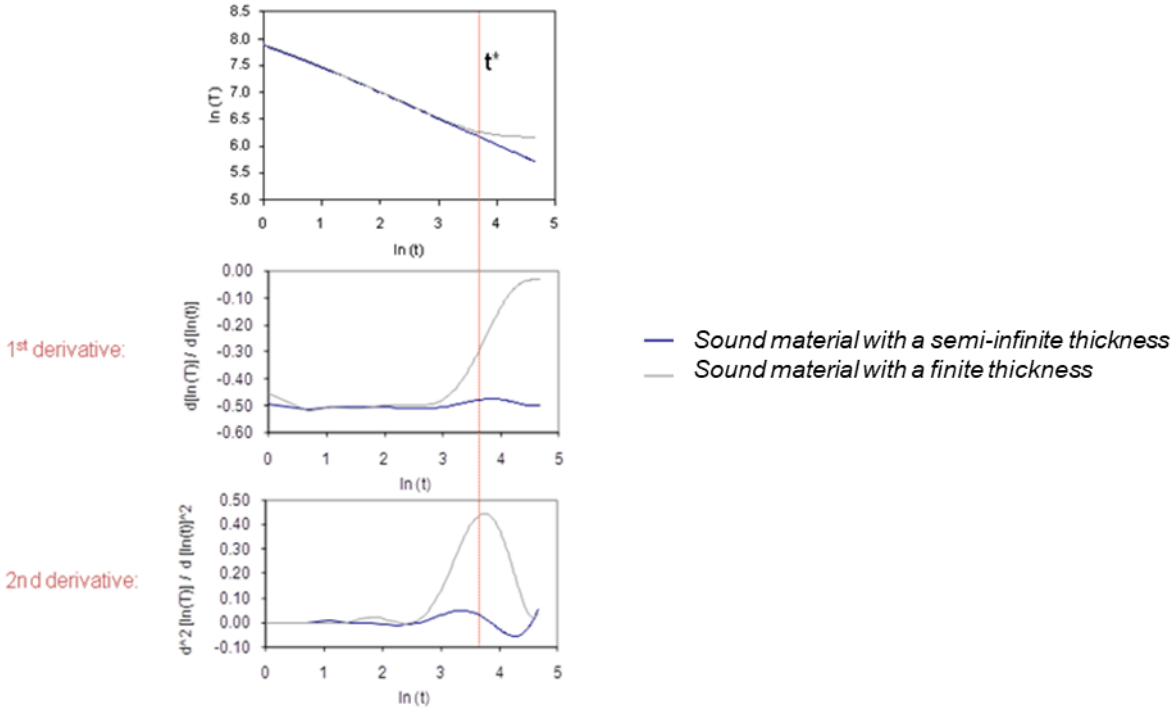

Fig. 4. *Principle of TSR 1st and and 2nd derivative [7]*

4. Parametric study

4.1. Influence of defect thickness

For a 3mm thick CFRP plate with a defect located at the middle of the thickness (cf. Figure 5), absolute contrast calculated on raw data tends to increase with the thickness of the defect. The time of initiation of the contrast (t_{grow}) is the same but the time of the maximum of contrast (t_{cmax}) increase with the thickness of the defect.

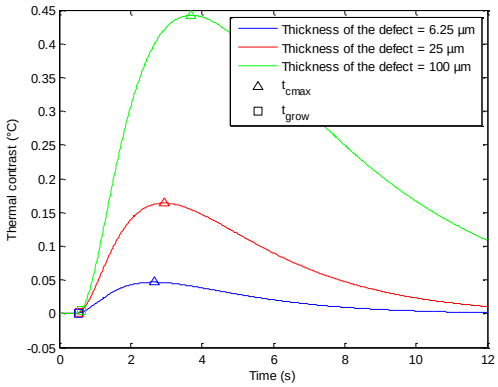

Fig. 5. *Absolute contrast for different thickness of defects located at a depth of 1.5 mm in a 3mm thick CFRP plate*

Results presented on Figure 6-(a) highlight that the value of the maximum of contrast decrease when the depth of the defect increase.

Figure 6-(b) allows to compare the values of the calculated t_{cmax} for the 3 defect thickness with the t_{cmax} values found in the literature. Even if it considers the defect thickness, the model proposed by Maldague tends to overestimate t_{cmax} and is quite far of calculated values while the model proposed by Cielo, without considering defect thickness, gives results close to the calculation for depth up to half of the thickness. However the shapes of these curves are not consistent.

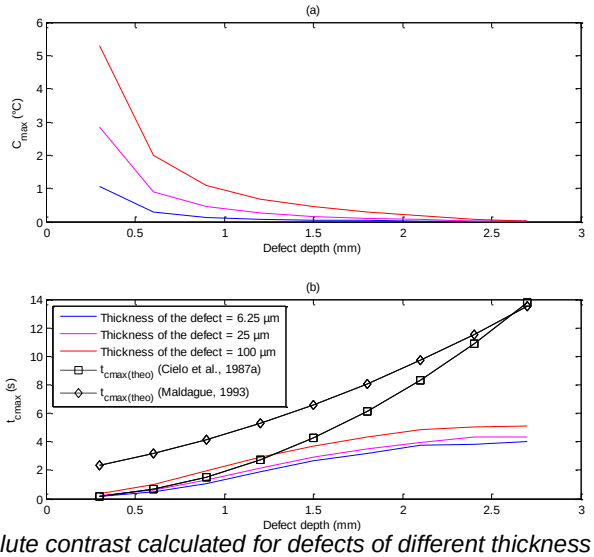

Fig. 6. *Maximum of absolute contrast calculated for defects of different thickness located at different depth. (a) Value of maximum of contrast. (b) Associated time of maximum of contrast.*

From results given on Figure 6-(a) and considering that a defect can be detected when absolute contrast is above *10.NETD*, one can estimate what could be the maximum depth of detection of a 10 to 100µm thick defect in a CFRP plate of 3mm. Figure 7 highlights that the thicker the defect, the better the detection. It also highlights that cooled cameras have better performances than uncooled cameras but, even with cooled camera, defect located in the second half of the thickness of the sample are difficult to detect with a good contrast on raw data, whatever their thickness.

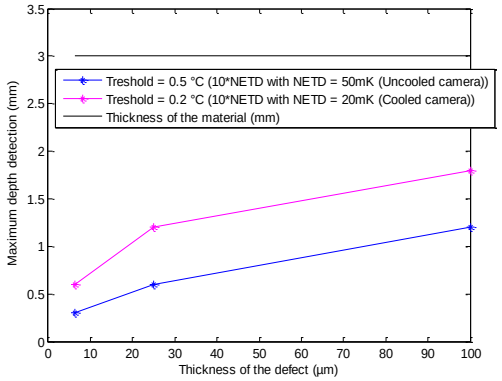

Fig. 7. *Maximum depth of detection estimated for a defect of different thickness in a CFRP plate of 3mm*

4.2. Influence of material thickness

For a given defect thickness (25µm) of a CRFP plate with a total thickness varying from 3 to 15mm, absolute contrast value calculated on raw data tends to decrease with increasing both the depth of the defect (Figure 8-(a)) and the thickness of the plate while t_{cmax} tends to increase (Figure 8-(b)).

It is interesting to note that, for a defect located at the same depth ratio, absolute contrast is smaller for thinner material. It is probably due to the fact that the thicker the material, the longer the temperature decrease will last to reach the steady state, having as a consequence to increase the contrast.

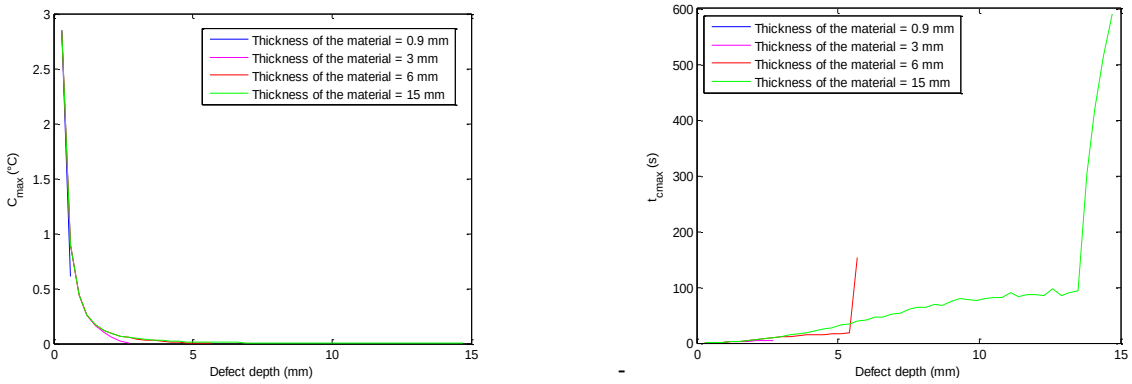

(a) Value of maximum of contrast *(b) Associated time of maximum of contrast*

Fig. 8. *Maximum of absolute contrast calculated according to different defect depth on material of different thickness*

Figure 9 highlights that, whatever the thickness of the material and the type of IR camera, it is complicated to detect a 25µm thick defect located at half the thickness of a CFRP plate if detection criteria is about *10.NETD*. One can see that it is better when considering just *1.NETD*. This induce that data averaging or signal processing would help to reduce the noise and improve detection. It is interesting to note that the thicker the material, the deeper detection is possible in absolute value,

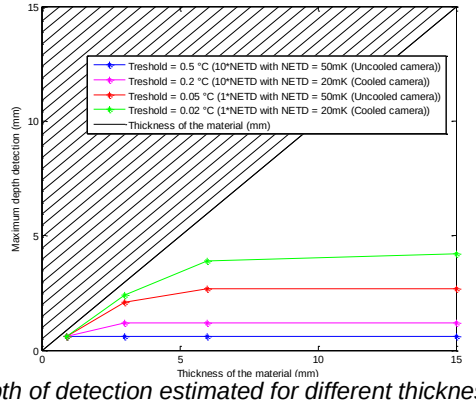

Fig. 9. *Maximum depth of detection estimated for different thickness of CFRP plate*

4.3. Influence of energy deposit

In order to estimate if the limitations observed in the section about influence of material thickness were due to a too low initial increase of temperature (~20°C), different levels of temperature increase have been simulated. One can observed on Figure 10 that the higher the energy deposit, the better the contrast. However this figure also highlight that, even for energy deposit that could possibly damage the material and considering a threshold corresponding *10.NETD* for a cooled camera, it is difficult to detect defects located in the second half of the thickness.

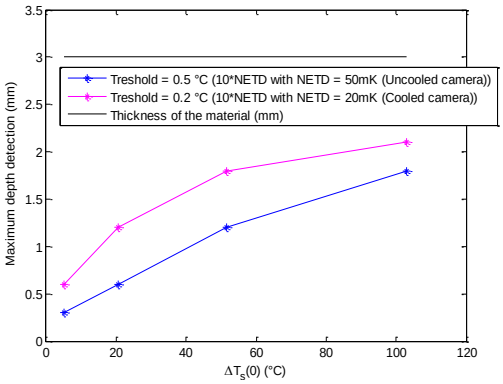

Fig. 10. *Maximum depth of detection estimated for different energy deposit on a 3mm thick CFRP plate*

In order to improve these performances, the effect of lock-in and signal processing (PPT and TSR) has then been evaluated for the same variation of energy.

When considering lock-in, one can observe that contrast on the amplitude value for the different lock-in frequencies is influenced by the energy deposit (Figure 11-(a)) whereas it is constant for the contrast on the phase value (Figure 11-(b)). On such a figure, f_{min}, f_b and f_{dec} (when phase contrast starts be different than 0 for decreasing lock-in frequencies) can be estimated. These frequencies are reported on Figure 12 for different levels of energy deposit and defect depth in a CFRP of 3mm. It is interesting to note that there is a very good correlation between:

- f_{dec}, the frequency when a beginning of contrast is observed, and $1/t^*$, when considering a material with a material thickness equivalent to the depth of the defect,
- $1/t_{cmax}$ proposed from Cielo and f_b.

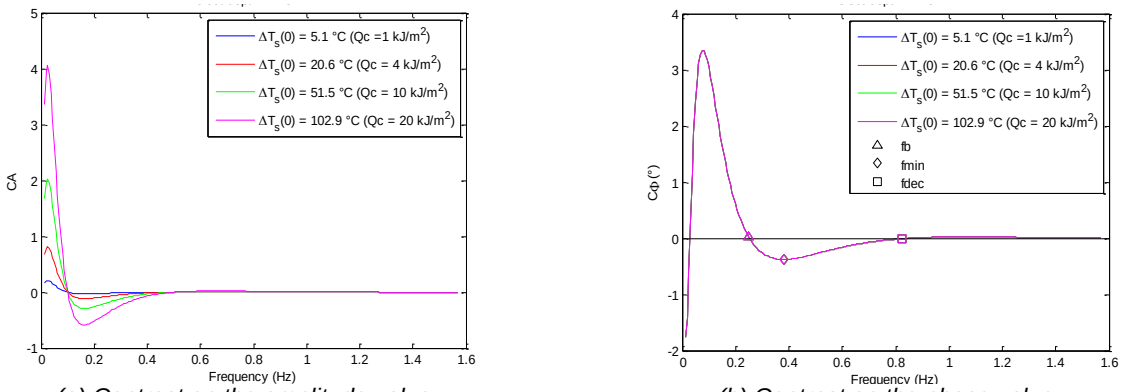

(a) Contrast on the amplitude value *(b) Contrast on the phase value*

Fig. 11. *Amplitude and phase contrast evolution according to lock-in frequency for different levels of energy deposit on a CFRP plate of 3mm with a defect located at the middle of the thickness*

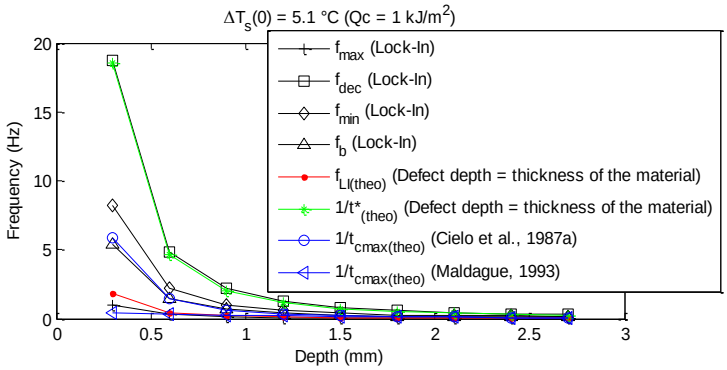

Fig. 12. *Comparison of key frequencies observed on contrast on the phase values with theoretical values of fLI, t* and tcmax for a defect located at different depth on a 3mm thick CFRP plate excited in Lock-in*

PPT analysis has also been performed on simulation data from flash thermography and the equivalent of all these frequencies have been estimated. Figure 13 then corresponds to the equivalent of figure 12 but with a PPT analysis on pulse excitation data. Results follow the same trends but the correlation is worth in the case of PPT data, possibly because the model is adapted for Dirac pulse while in this study the flash is simulated by a pulse of 10ms that is too large to behave like a Dirac.

Figure 14 highlights that the behaviour on First and on the Second Derivative are the same for the different energy deposited. All these results tend to promote data processing that allow an early detection of the defect that help to capture some contrast for deeper defects.

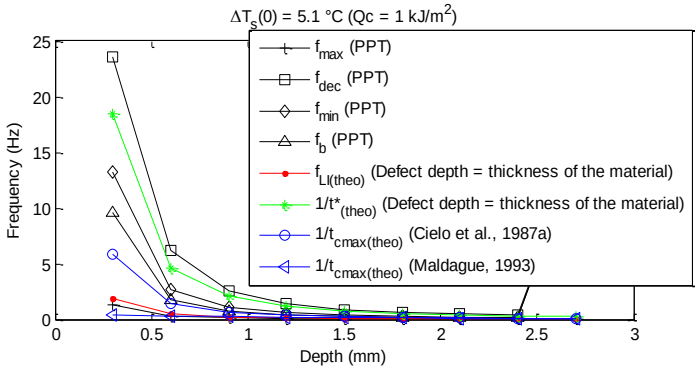

Fig. 13. *Comparison of key frequencies observed on contrast on the phase values with theoretical values of f_{LI}, t* and t_{cmax} for a defect located at different depth on a 3mm thick CFRP plate excited in pulse mode and analysed in PPT*

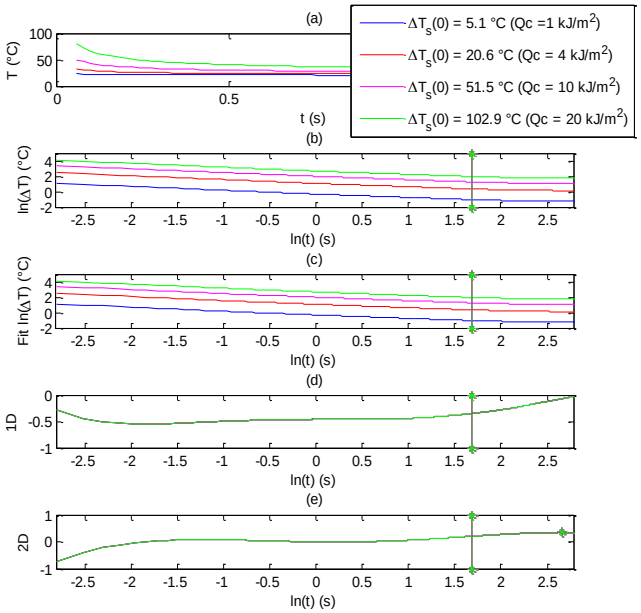

Fig. 14. TSR curves for different energy deposit *for a defect located at different depth on a 3mm thick CFRP plate excited in pulse mode. (a) Raw data, (b) Logarithm of temperature difference with initial temperature vs. logarithm of time, (c) Fit of (b), (d) First Derivative curve, (e) Second Derivative curve*

5. Conclusions

The aim of this study was to allow Safran to have a better knowledge of the key parameters for Flash Thermography inspection.

Based on these results and industrial perspectives, Safran considered flash thermography with cooled camera and TSR processing to be the best candidate to inspect composites panels. These results also allowed to define precisely the acquisition parameters (energy deposited, acquisition duration…) to be used regarding the material diffusivity and thickness.

By a better knowledge of the characteristic times (cf. figure 15) observed on the signal, this study has also been used to optimise analysis conditions for the inspectors in production.

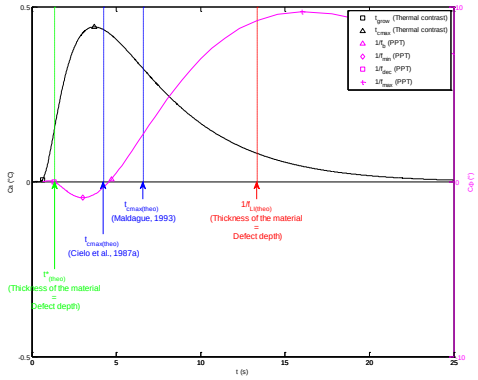

Fig. 15. *Comparison of characteristic times given in the literature vs. absolute thermal contrast and phase contrast on simulated data on CFRP plates*

REFERENCES

[1] Marin J. Y., ITsimul20.htm, Tutoriel du logiciel ITsimul2, 2009-2011

[2] Theory and practice of infrared technology for nondestructive testing, Xavier P.V. MALDAGUE, Wiley series in microwave and optical engineering Kai Chang, Series editor, 30 avril 2001

[3] Cielo P., Maldague X., Déom AA. Lewak R., Thermographic nondestructive evaluation of industrial matetrials and structures, Materials Evaluation, 1987

[4] Busse G., Lockin-Thermography: Principles, NDE-applications, and trends, Proceedings of 12th Quantitative InfraRed Thermography conference, Bordeaux (France), 2014.

[5] Guibert S., La thermographie infrarouge à détection synchrone appliquée aux matériaux composites, Mémoire présenté à la Faculté des études supérieures de l'Université Laval dans le cadre du programme de Maîtrise en génie électrique pour l'obtention du grade de Maître des Sciences (M.Sc.), 2007

[6] Shepard S., System for generating thermographic images using thermographic signal reconstruction, US6751342B2, 2004

[7] Shepard S., Advances in active thermography for inspection of CFRP and GFRP components, TWI VoyageIR training document, 2014